The onset of the spring phytoplankton bloom in the coastal North Sea supports the Disturbance Recovery Hypothesis

Ricardo González-Gil[1*], Neil S. Banas[1], Eileen Bresnan[2], Michael R. Heath[1]

[1]Department of Mathematics and Statistics, University of Strathclyde, 26 Richmond Street, Glasgow, G1 1XH, UK
5   [2]Marine Scotland Science, Marine Laboratory, 375 Victoria Road, Aberdeen, AB11 9DB, UK

Correspondence to: Ricardo González-Gil (rgonzalezgil@gmail.com)

Abstract. The spring phytoplankton bloom is a key event in temperate and polar seas, yet the mechanisms that trigger it remain under debate. Some hypotheses claim that the spring bloom onset occurs when light is no longer limiting, allowing
10   phytoplankton division rates to surpass a critical threshold. In contrast, the Disturbance Recovery Hypothesis (DRH) proposes that the onset responds to an imbalance between phytoplankton growth and loss processes, allowing phytoplankton biomass to start accumulating, and this can occur even when light is still limiting. Although many studies have shown that the DRH explains the spring bloom onset in oceanic waters, it is less certain whether and how it also applies to coastal areas. To address this question at a coastal location in the Scottish North Sea, we combined 21 years (1997–2017) of weekly in situ
15   data with meteorological information. The onset of phytoplankton biomass accumulation occurred around the same date each year, 16 ± 11 days (mean $\pm$ SD) after the winter solstice, when light limitation for growth was strongest. Also, negative and positive biomass accumulation rates (r) occurred respectively before and after the winter solstice at similar light levels. The seasonal change from negative to positive r was mainly driven by the rate of change in light availability rather than light itself. Our results support the validity of the DRH for the studied coastal region and suggest its applicability to other coastal
20   areas.

1   Introduction

The spring bloom is a major seasonal feature of temperate and polar seas and plays significant ecological and biogeochemical roles (Townsend et al., 1994). Although scientists generally agree that this event corresponds to large accumulations of phytoplankton biomass, no consensus has been reached on how it is initiated, even after more than a
25   century of research (Behrenfeld and Boss, 2014; Behrenfeld and Boss, 2018). Despite this ongoing discussion, all current theories attempt in essence to understand how phytoplankton biomass starts to accumulate; i.e., how the biomass accumulation rate (r), which is the difference between phytoplankton division and loss rates (μ and l, respectively), becomes positive.

The more traditional school of thought assumes that the spring bloom is triggered when the winter light limitation relaxes to
a point that allows μ to surpass a critical threshold (Behrenfeld and Boss, 2014; Behrenfeld and Boss, 2018). To this pure
bottom-up view belong for instance the famous Critical Depth Hypothesis (CDH, Sverdrup, 1953) and Critical Turbulence
Hypothesis (CTH, Huisman et al., 1999). An alternative framework focuses on processes that lead to positive r by disrupting
the equilibrium between phytoplankton division and loss processes, especially grazing and virus infections, and this
disruption can occur even when light is still limiting. To this other view belongs the Disturbance Recovery Hypothesis
(DRH, Behrenfeld et al., 2013; Behrenfeld and Boss, 2014).

The DRH suggests that positive r observations in early winter are possible if the mixed layer deepening has a stronger
negative impact on l, by reducing plankton encounter rates through dilution effects, than on μ, by increasing light limitation
(Behrenfeld, 2010; Behrenfeld and Boss, 2018). Also, in opposition to the other school of thought, the DRH states that r
follows the rate of change in division rates ($d\mu/dt$) rather than μ itself (Behrenfeld et al., 2013; Behrenfeld and Boss, 2018).
According to this idea, an acceleration in μ impacts the μ–l balance, allowing phytoplankton to start blooming (i.e., to start
accumulating biomass).

Although the DRH is supported by many satellite and field observations in oceanic waters (Behrenfeld and Boss, 2018), we
are not aware of any study showing how this hypothesis explains the spring bloom onset in coastal areas. Although these
areas cover a small percentage of the ocean surface, they are among the most productive in the world (Mann, 2009) and
provide important ecosystem services (Barbier, 2017). However, they are also under intense human pressure, as the global
population is highly concentrated along the coastline (Cloern et al., 2016). Mignot et al. (2018) suggested that in coastal
ecosystems, low variations in the mixed layer depth would decrease the importance of plankton dilution effects, probably
leading to no phytoplankton biomass accumulation in winter. Nevertheless, according to the DRH, an early μ acceleration
driven for example by a seasonal improvement in light conditions (i.e., by an accelerating increase in light availability) could
still trigger a phytoplankton biomass accumulation in winter. This is plausible considering that coastal waters usually have
high nutrient and turbidity levels during winter and spring (Mann, 2009), making light the main limiting factor for
phytoplankton growth, especially at high latitudes with low surface light intensities and stormy weather.

We combined 21 years of weekly in situ data (1997–2017) and meteorological information to study how the spring
phytoplankton bloom is initiated in the Scottish coastal North Sea. In particular, we addressed the questions: 1) Does the
spring bloom start in winter in the absence of a deepening in the mixed layer? 2) Is light availability a main driver of the
process? And 3) Does the DRH hold true?

2 Material and methods

2.1 Monitoring site and environmental variables

60 The time series analyzed was collected at the Marine Scotland Scottish Coastal Observatory monitoring site at Stonehaven (56° 57.8′ N, 02° 06.2′ W, northwestern North Sea), a 48 m depth coastal station located 5 km offshore (Bresnan et al., 2016). This station has been sampled at a weekly frequency (weather permitting) since January 1997. In this study, data collected until December 2017 were used (Marine Scotland Science, 2018). At a local scale, this coastal area is affected by strong tidal currents and winds, leading to a well-mixed water column for most of the year (Bresnan et al., 2016).

65 Different physicochemical variables were sampled to characterize the water column environment. Salinity, Total Oxidized Nitrogen (TOxN), and other nutrient concentrations were measured from water collected at surface and bottom depths (0–5 m and ~45 m, respectively) using Niskin bottles. These bottles were also equipped with digital reversing thermometers to record water temperature. A Secchi disk was used since 2001 to estimate light attenuation (K_d) of the water column (Supplementary Note 1 and Figure S1). Also, water was sampled using a 10 m Lund tube to obtain integrated surface

70 chlorophyll '*a*' (Chl) concentrations and, since 2000, phytoplankton community counts using an inverted microscope at x200 magnification (taxa with mean cell diameters generally > 10 μm, Table S1). For a full description of sampling and laboratory procedures, see Bresnan et al. (2016). Since 2015, Lund tube water samples were also analyzed using a BD Accuri™ C6 flow cytometer to estimate pico-, and nanophytoplankton abundances, which rarely exceeded 10 μm cell diameter (for a full description of the flow cytometry methodology, see Tarran and Bruun, 2015).

75 As light is one of the main limiting factors for phytoplankton growth in coastal waters of the North Sea (Reid et al., 1990), we also estimated daily Photosynthetic Active Radiation (PAR) at the sea surface and within the water column (Supplementary Notes 2–3 and Figures S2–3). First, we estimated surface PAR (PAR_{Sfc}) using sunshine durations recorded at the Dyce meteorological station (57° 12.3' N, 2° 12.2' W, Met Office, 2012), located 27.6 km away from the Stonehaven site. Then, using K_d and PAR_{Sfc} estimations, we calculated average attenuated PAR (PAR_{Att}) for the top 10 m layer (where

80 phytoplankton samples were collected) and for the entire water column ($PAR_{Att,10}$ and $PAR_{Att,48}$, respectively). Without using vertical profiles of physical variables, we could not estimate the exact mixing layer depth, which determines how deep phytoplankton can be moved away from surface layers and, consequently, the amount of PAR they receive. Thus, we calculated $PAR_{Att,10}$ and $PAR_{Att,48}$ to estimate the range within the actual PAR experienced by phytoplankton occurs. Both PAR_{Sfc} and the two PAR_{Att} are reported in μmol m^{-2} s^{-1}.

85 2.2 Phytoplankton biomass accumulation rates (*r*) and spring bloom parameters

The analysis of the spring phytoplankton bloom requires estimating changes through time in biomass accumulation rates, *r* (Behrenfeld and Boss, 2018). We first transformed Chl into carbon (C) biomass of the entire phytoplankton community

(C_{phyto}, mg C m^{-3}) using an average seasonality of C:Chl ratios, estimated by combining microscopy and flow cytometry counts with cell data from the literature (Supplementary Notes 4–5, Figure S4 and Tables S1–3).

90 Once C_{phyto} was estimated, we calculated r between two sampling dates separated by a period of time ($\Delta t = t_2 - t_1$) as:

$$r = \frac{\ln(C_{phyto,2}) - \ln(C_{phyto,1})}{\Delta t} \qquad (1)$$

To filter short-term variations in phytoplankton biomass and focus on the main winter–spring phenology pattern, we chose Δt to match the average e-folding timescale (T_e) of the spring bloom (Mignot et al., 2018), calculated as:

95

$$T_e = \frac{t_{max\,C} - t_{min\,C}}{\ln(C_{phyto\,max}) - \ln(C_{phyto\,min})} \qquad (2)$$

where $t_{min\,C}$ and $t_{max\,C}$ correspond respectively to the date when C_{phyto} was minimum and maximum between December and May (we considered $t_{max\,C}$ as the timing of the spring bloom peak). The average T_e was 32.1 ± 9.0 days (mean ± SD) and thus, we selected t_2 to be the fourth sampling date after t_1 ($\Delta t = 31.4 \pm 8.4$ days). The possibility that using an average
100 C:Chl seasonality artificially modified the general seasonal r pattern was discarded (Figure S5).

We also calculated the spring bloom onset (t_0), defined as the first date after November when r was positive for at least 15 consecutive days, and the date when r was maximum between December and May ($t_{max\,r}$). Before calculating t_0 and $t_{max\,r}$, r was linearly interpolated between sampling dates to generate daily r estimates. Also, other variables were linearly interpolated to estimate environmental conditions at t_0 and $t_{max\,r}$.

105 ## 2.3   Statistical analysis

Seasonal mean environmental conditions were described using generalized additive models (GAMs) with a cyclic cubic regression spline (Wood, 2017) to identify potential factors driving the spring bloom onset. Then, to test which type of hypothesis better explains the spring bloom onset, we correlated r with average PAR or average rates of change in PAR

(dPAR/dt) around t_0. PAR and dPAR/dt were averaged from t_1 to $t_2 - 1$ day (see Eq. 1), as sampling generally occurred in
the morning (09:30 ± 1.45 h, mean ± SD). For the correlations, we excluded averages estimated with fewer than 15 PAR
values.

All analyses and plots were performed in R v4.0.3 (R Core Team, 2020), using the Rstudio interface v1.3.1093 (Rstudio
Team, 2020) and the tidyverse packages v1.3.0 (Wickham et al., 2019).

3 Results

3.1 Interannual variability and seasonality of the spring bloom

Phytoplankton biomass showed a clear seasonal pattern where the spring bloom was a major feature (Figure 1 and Figure 2).
The analysis of bloom parameters revealed that although the spring bloom onset (t_0) had low interannual variability
(January 6th ± 11 days, mean ± SD), the timing of maximum r ($t_{max\,r}$, April 9th ± 18 days) and bloom peak ($t_{max\,C}$,
May 8th ± 14 days) changed more from year to year. The maximum r and peak biomass showed the strongest interannual
variability (0.070 ± 0.020 d^{-1} and 309 ± 125 mg C m^{-3} on average, respectively).

Inspection of the environmental conditions during the spring bloom revealed a complex scenario (Figure 2), with fresh water
influence (as shown by the marked lower surface than bottom salinity in some dates), an absence of thermal stratification (as
there is almost no difference between surface and bottom temperatures), and strong light attenuation, especially during
January–March. We observed a phytoplankton succession during the spring bloom (Figure 3), dominated by small (< 10 µm)
taxa in winter (approximately November–March), and then by larger diatoms and dinoflagellates.
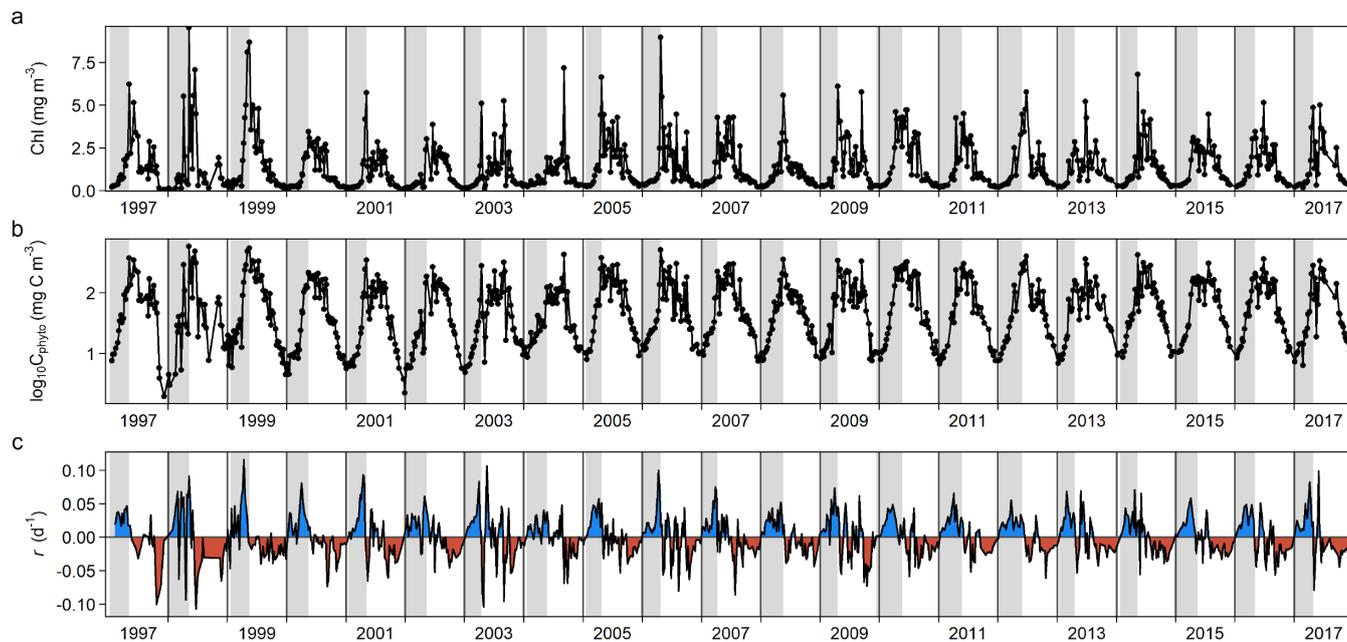
Figure 1. Changes through time in (a) chlorophyll 'a' (Chl) concentration, (b) log-transformed phytoplankton biomass (C_{phyto}) concentration, and (c) biomass accumulation rate (r). Blue and red areas in (c) indicate positive and negative r, respectively. Vertical gray stripes correspond to the estimated spring bloom span each year, from t_0 to $t_{max\,C}$ (see Methods). For 1997, we used the average date of the spring bloom onset estimated using the rest of the time series (January 6th).
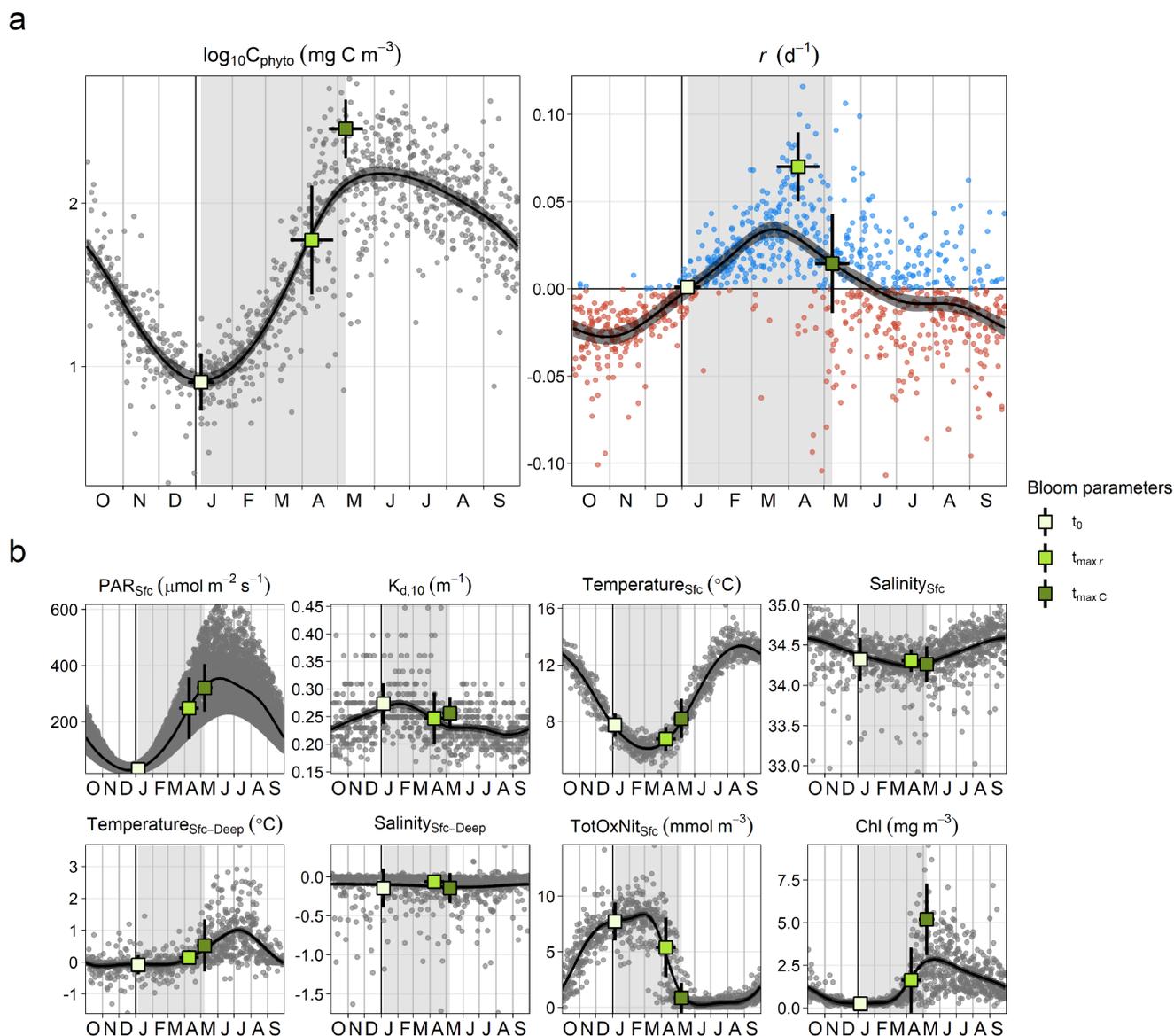
Figure 2. Seasonal cycle of physicochemical and phytoplankton variables. (a) log-transformed phytoplankton biomass (C_{phyto}) concentration and biomass accumulation rate (r), which were used to estimate the timing of the spring bloom parameters: the spring bloom onset (t_0), the maximum r ($t_{max\ r}$), and the spring bloom peak ($t_{max\ C}$). (b) Surface Photosynthetic Active Radiation (PAR), attenuation coefficient for the 0–10 m layer ($K_{d,\ 10}$), surface temperature and salinity (Temperature$_{Sfc}$ and Salinity$_{Sfc}$, respectively), difference between surface and bottom temperature and salinity (Temperature$_{Sfc-Deep}$ and Salinity$_{Sfc-Deep}$, respectively), total surface oxidized nitrogen concentration (TotOxNit$_{Sfc}$), and chlorophyll 'a' (Chl) concentration. Dots (gray or blue and red for positive and negative r, respectively) correspond to individual values. Black curves and the associated gray shaded areas define respectively the average seasonality and 95% confidence interval based on a generalized additive model (GAM). Vertical gray stripes mark the average spring bloom span. Average ± SD timing of different bloom parameters and associated average ± SD environmental conditions are also shown (squares and corresponding error bars).
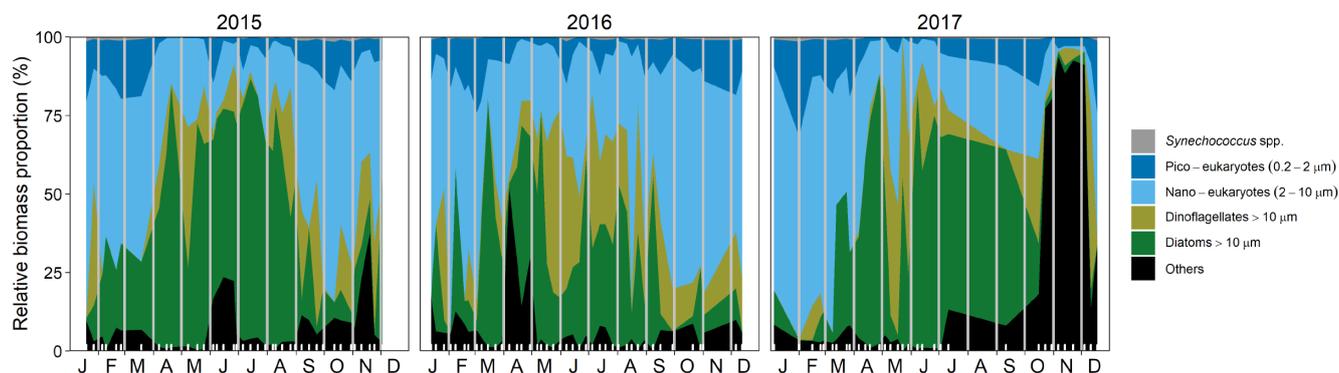
Figure 3. Seasonal changes in the proportional biomass of different phytoplankton groups from 2015 to 2017. The "Others" category combines three phytoplankton groups identified using a flow cytometer: Coccolithophores, Cryptophytes and *Phaeocystis* spp. single cells. The large proportional biomass of this category in October–December 2017 corresponds mainly to a *Phaeocystis* spp. bloom. Inner white tick marks on the x-axis indicate those dates when data were collected, and data gaps at the beginning and end of each year appear as vertical white stripes.

3.2 Effect of light on the spring bloom onset

The estimated t_0 occurred on average 16 ± 11 days after the winter solstice (Figure 2), when surface PAR was still very low (29.34 ± 11.16 µmol m^{-2} s^{-1} on average), light attenuation was high (average $K_{d,10}$ of 0.273 ± 0.037 m^{-1}), and the water column was homogeneous (difference between surface and bottom temperature and salinity was on average -0.09 ± 0.30 °C and -0.15 ± 0.25, respectively) (Figure 2). Thus, although during the bloom onset nutrient concentrations were high (surface TOxN concentration was on average 7.71 ± 1.71 mmol m^{-3}), light limitation for phytoplankton growth was strongest in the year. Also, we observed that the r seasonal cycle increased from maximum negative rates in October–November to maximum positive ones in March–April (Figure 2). However, for same time distances before and after the winter solstice from November to February, average light availability and nutrient conditions were similar (Figure 2 and Figure 4).

In winter, for a period extending 60 days before and after the winter solstice, we observed that r was better correlated with the rate of change in surface and attenuated PAR (dPAR/dt) than with PAR itself (Figure 4). Specifically, we found that the proportion of variance in r explained by surface and attenuated dPAR/dt was 0.41 and 0.50, respectively, but the proportion explained by PAR itself was almost zero. The similar effect of surface and attenuated dPAR/dt on r indicates that, at a seasonal scale, surface PAR is the major factor driving PAR changes in time within the water column. However, Figure 4 shows that water attenuation has a strong impact on the average light levels experienced by phytoplankton. In particular, for the period analyzed, average PAR levels assuming a homogeneous water column (PAR$_{Att,48}$) remained below 10 µmol m^{-2} s^{-1}.
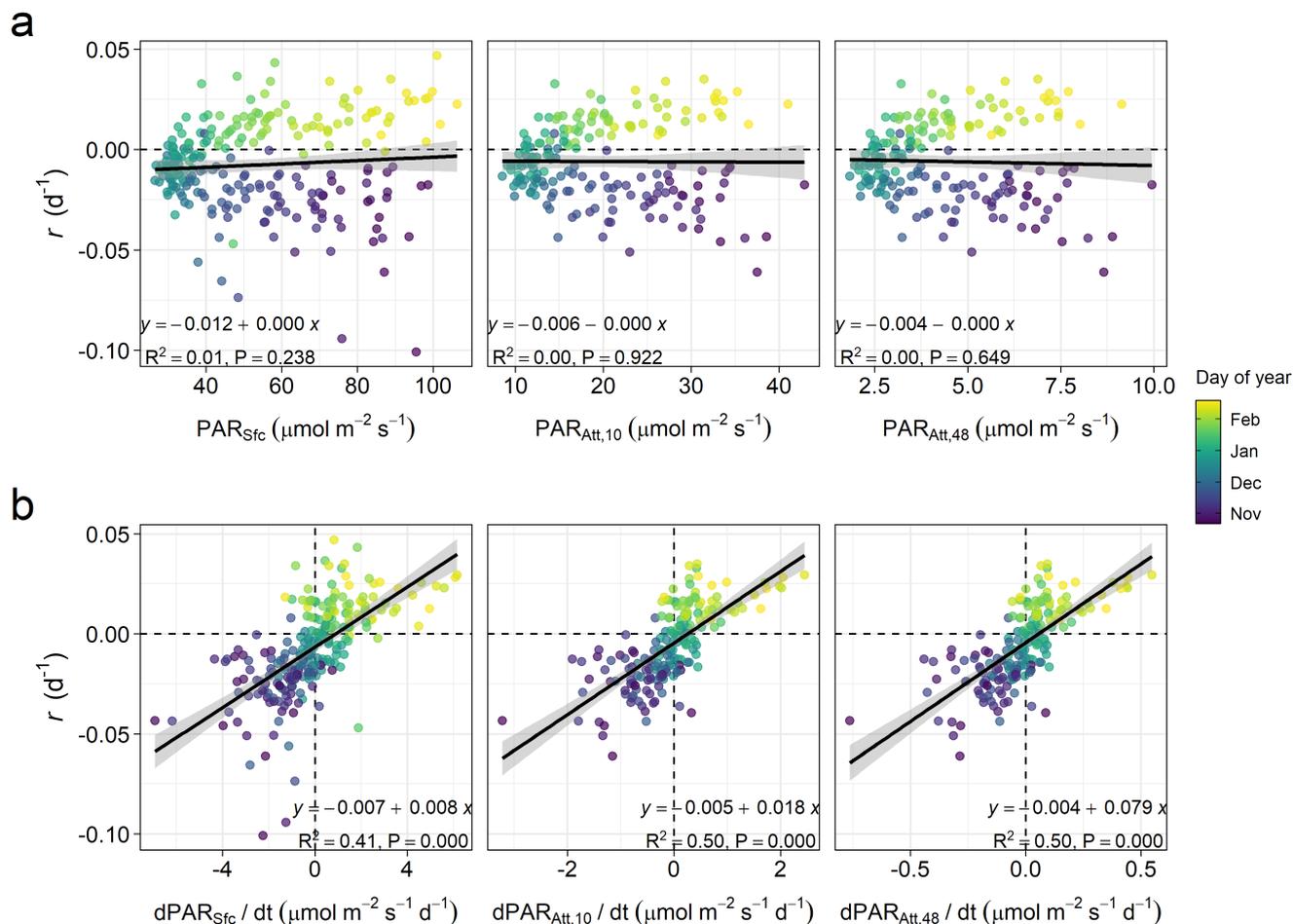
Figure 4. Linear relationships in winter (60 days before and after the winter solstice) between (a) phytoplankton biomass accumulation rate (r) and average Photosynthetic Active Radiation (PAR) at the sea surface (PAR_{Sfc}), for the 0–10 m layer (the layer where phytoplankton was sampled, $PAR_{Att,10}$), or for the entire water column (i.e., 0–48 m depth, $PAR_{Att,48}$), or between (b) r and average rates of change in PAR ($dPAR_{Sfc}/dt$, $dPAR_{Att,10}/dt$, and $dPAR_{Att,48}/dt$). The shaded area represents the 95% confidence interval associated with the estimated linear correlation (black line). The equation, proportion of variance explained (R^2), and p-value (P) of the relationships are shown. Horizontal and vertical dashed lines indicate zero rates.

4   Discussion

The spring bloom onset occurred just after the winter solstice in most years at the studied coastal site. This remarkable regularity contrasts with the larger interannual variability in timing and especially in magnitude of the maximum biomass accumulation rate (r) and bloom peak biomass. The observed early winter initiation contradicts Mignot et al.'s (2018) expectations for waters without the dilution effects associated with the mixed layer deepening, indicating the operation of other processes. We found that changes from negative to positive biomass accumulation rates around the winter solstice followed seasonal variations in dPAR/dt rather than PAR itself.

During winter, surface nutrient concentrations remained high and light was probably the main limiting factor for phytoplankton growth at Stonehaven. Although this is the norm in most temperate and polar areas (Simpson and Sharples, 2012; Behrenfeld and Boss, 2014), winter light levels might be especially limiting in the Scottish North Sea due to several factors: its high latitude, frequent storminess, and strong light attenuation due to elevated turbidity (Reid et al., 1990), which might increase in the future (Wilson and Heath, 2019). Also, the observed vertical homogeneity of the water column probably indicates an intense turbulent mixing that keeps phytoplankton cells moving between surface and bottom layers, throughout the vertical light gradient (Reid et al., 1990; Simpson and Sharples, 2012). Consequently, winter PAR levels for the entire water column are well below optimal irradiances for maximum growth rates in most phytoplankton taxa (Edwards et al., 2015). Therefore, it could be surprising that the spring bloom onset usually occurred just after the winter solstice, when phytoplankton division rates (μ) suffer the strongest light limitation. Even more, r was negative during the weeks before the solstice and changed to positive some days after the solstice. Thus, r cannot just depend on μ, as mean seasonal PAR levels (and probably the associated μ) are similar at same time distances before and after the winter solstice. These observations contradict the expectations of the more traditional hypotheses about the spring bloom onset (e.g., Sverdrup, 1953).

Another consequence of the low winter light experienced by phytoplankton is that μ would be expected to respond almost linearly to changes in PAR (Edwards et al., 2015). Thus, the positive linear relationship between r and dPAR/dt estimated around the solstice, mostly driven by seasonal changes in surface PAR, is probably reflecting the covariation of r with $d\mu/dt$. This relationship between r and $d\mu/dt$ has also been observed in oceanic waters of temperate and polar regions (see for example Behrenfeld, 2014; Behrenfeld et al., 2016; Arteaga et al., 2020) and fits within the framework of the Disturbance Recovery Hypothesis (DRH, Behrenfeld et al., 2013; Behrenfeld and Boss, 2014). Such relationship requires a tight coupling between division and loss processes (Behrenfeld and Boss, 2018). In particular, the dynamics of small phytoplankton (< 10 µm) are tightly coupled with those of microzooplankton grazers due to their fast ingestion and growth rates (Hansen et al., 1997; Haraguchi et al., 2018), allowing them to consume most phytoplankton primary production in the ocean, including coastal habitats (Calbet and Landry, 2004). Also, a Holling III functional response seems to best describe the grazing behavior of microzooplankton (Liu et al., 2021), which might be key at low winter food concentrations to allow

phytoplankton biomass to accumulate (Freilich et al., 2021). At Stonehaven, we observed that small phytoplankton dominated the winter community biomass, as also occurs in other temperate oceanic and coastal areas (see for instance Haraguchi et al., 2018; Bolaños et al., 2020).

205 In addition to light variations, other factors might contribute to the observed seasonal pattern in biomass accumulation around the spring bloom onset. For instance, Rose and Caron (2007) showed that decreasing temperatures impact more negatively microzooplankton than phytoplankton growth rates (although see Chen et al., 2012), which could favor the bloom initiation. However, we observed that water temperatures decrease until a seasonal minimum around two months after r becomes positive, suggesting a lesser role than light variations. Also, the southward coastal flow characteristic of the study

210 area (León et al., 2018) could contribute to the bloom onset delay with respect to the winter solstice (16 days on average) by bringing waters with lower phytoplankton biomass concentrations. This could occur in winter as the further north the spring bloom occurs in the North Sea, the longer it takes to reach a certain biomass level (Henson et al., 2009). Additionally, although we analyzed the spring bloom as an aggregate community phenomenon, we recognize the importance of the seasonal phytoplankton succession (Lewandowska et al., 2015). In particular, we hypothesize that to keep μ accelerating in

215 response to the seasonal light improvement, it is necessary that a succession of species with traits suited to each new environmental condition occurs during the bloom progression (Behrenfeld et al., 2016), consistent with the complex changes in group composition observed (Figure 3).

One limitation of our study is using an average seasonality of C:Chl ratios to estimate phytoplankton biomass for all years, as these ratios change in response to environmental conditions (Geider, 1987). Alternatively, some studies have proposed

220 models that calculate C:Chl based on environmental conditions (e.g., Geider, 1987; Cloern et al., 1995). This approach is not possible in our case as we cannot determine the mixing layer depth in summer and, consequently, the amount of light experienced by phytoplankton. Nevertheless, for the winter period analyzed, when the mixing layer usually extends the entire water column, biomass estimated assuming a homogeneous water column and using C:Chl models (Geider, 1987; Cloern et al., 1995) were very similar to those calculated using a constant C:Chl seasonality (Figure S6). Also, measuring

225 PAR in situ would have improved the accuracy of our PAR estimations. However, we think our results were not importantly affected by this as we were mainly interested in the seasonal pattern around the spring bloom onset. Nevertheless, disentangling local from larger-scale processes is probably crucial to deeply understand the intra and interannual variability of the whole spring bloom in this complex hydrographic ecosystem (Blauw et al., 2018). This could be achieved through dynamic 3-D models that consider advection and incorporates processes at very different spatiotemporal scales.

230

5   Conclusions

Overall, we showed that the spring bloom onset in a generally well-mixed coastal location of the North Sea supports the Disturbance Recovery Hypothesis (DRH). Nevertheless, the mechanisms described in other competing hypotheses such as the Critical Depth Hypothesis (CDH, Sverdrup, 1953) or the Critical Turbulence Hypothesis (CTH, Huisman et al., 1999)
235   might contribute to the spring bloom development in later stages by a fast (albeit temporary) increase in both light availability and division rates (Morison et al., 2020; Mojica et al., 2021), as described for oceanic waters by Mignot et al. (2018) and Yang et al. (2020). Our results suggest that the DRH might also explain the spring bloom onset in other coastal areas or lakes, and that this onset can occur in early winter despite the absence of a mixed layer deepening.

6   Data availability

240   The datasets analyzed in this study (doi: 10.7489/1761-1) are available in the Marine Scotland website (https://data.marine.gov.scot/dataset/scottish-coastal-observatory-stonehaven-site). Metadata for the sampling site and methods used can be found in Bresnan et al. (2016)

7   Author contribution

R.G.-G. and N.S.B. designed and conceived the study. E.B. and M.R.H. coordinated sample collection and analysis. All
245   authors participated in the data analysis and contributed to writing the manuscript.

8   Competing interests

The authors declare that they have no conflict of interest.

9   Acknowledgements and funding

We thank all staff involved in collecting, analyzing and QCing Stonehaven data since 1997 and Glen Tarren in Plymouth
250   Marine Laboratory, who analyzed the flow cytometry data. We are especially grateful to P. León, J. Hindson, M. Machairopoulou, P. Walsham, B. Chen, A. Rivera, F. González Taboada and C. Cáceres for their insightful comments. Also, we acknowledge the information provided by the National Meteorological Library and Archive – Met Office, UK (© Crown Copyright 2020). R.G.-G. was supported by a Marie Curie-COFUND grant (ACA17-05) from the Government of the Principality of Asturias and the European Commission. The Scottish Coastal Observatory is funded by the Scottish
255   Government service level agreement ST05a. Flow cytometry analysis was funded by Scottish Government ROAME ST0160.

10 References

Arteaga, L. A., Boss, E., Behrenfeld, M. J., Westberry, T. K., and Sarmiento, J. L.: Seasonal modulation of phytoplankton biomass in the Southern Ocean, Nat. Commun., 11, 5364, doi: 10.1038/s41467-020-19157-2, 2020.

260 Barbier, E. B.: Marine ecosystem services, Curr. Biol., 27, R507-R510, doi: 10.1016/j.cub.2017.03.020, 2017.

Behrenfeld, M. J.: Abandoning Sverdrup's Critical Depth Hypothesis on phytoplankton blooms, Ecology, 91, 977-989, doi: 10.1890/09-1207.1, 2010.

Behrenfeld, M. J.: Climate-mediated dance of the plankton, Nat. Clim. Change, 4, 880-887, doi: 10.1038/nclimate2349, 2014.

Behrenfeld, M. J. and Boss, E. S.: Resurrecting the ecological underpinnings of ocean plankton blooms, Annu. Rev. Mar. Sci., 6, 167-194, 265 doi: 10.1146/annurev-marine-052913-021325, 2014.

Behrenfeld, M. J. and Boss, E. S.: Student's tutorial on bloom hypotheses in the context of phytoplankton annual cycles, Glob. Change Biol., 24, 55-77, doi: 10.1111/gcb.13858, 2018.

Behrenfeld, M. J., Doney, S. C., Lima, I., Boss, E. S., and Siegel, D. A.: Annual cycles of ecological disturbance and recovery underlying the subarctic Atlantic spring plankton bloom, Glob. Biogeochem. Cycles, 27, 526-540, doi: 10.1002/gbc.20050, 2013.

270 Behrenfeld, M. J., Hu, Y., O'Malley, R. T., Boss, E. S., Hostetler, C. A., Siegel, D. A., Sarmiento, J. L., Schulien, J., Hair, J. W., Lu, X., Rodier, S., and Scarino, A. J.: Annual boom–bust cycles of polar phytoplankton biomass revealed by space-based lidar, Nat. Geosci., 10, 118, doi: 10.1038/ngeo2861, 2016.

Blauw, A. N., Benincà, E., Laane, R. W. P. M., Greenwood, N., and Huisman, J.: Predictability and environmental drivers of chlorophyll fluctuations vary across different time scales and regions of the North Sea, Prog. Oceanogr., 161, 1-18, doi: 275 10.1016/j.pocean.2018.01.005, 2018.

Bolaños, L. M., Karp-Boss, L., Choi, C. J., Worden, A. Z., Graff, J. R., Haëntjens, N., Chase, A. P., Della Penna, A., Gaube, P., Morison, F., Menden-Deuer, S., Westberry, T. K., O'Malley, R. T., Boss, E., Behrenfeld, M. J., and Giovannoni, S. J.: Small phytoplankton dominate western North Atlantic biomass, ISME J., doi: 10.1038/s41396-020-0636-0, 2020.

Bresnan, E., Cook, K., Hindson, J., Hughes, S., Lacaze, J.-P., Walsham, P., Webster, L., and Turrell, W. R.: The Scottish Coastal 280 Observatory 1997-2013. Part 2 - Description of Scotland's Coastal Waters, Scott. Mar. Freshw. Sci., 7, 1-278, doi: 10.7489/1881-1, 2016.

Calbet, A. and Landry, M. R.: Phytoplankton growth, microzooplankton grazing, and carbon cycling in marine systems, Limnol. Oceanogr., 49, 51-57, doi: 10.4319/lo.2004.49.1.0051, 2004.

Chen, B., Landry, M. R., Huang, B., and Liu, H.: Does warming enhance the effect of microzooplankton grazing on marine phytoplankton 285 in the ocean?, Limnol. Oceanogr., 57, 519-526, doi: 10.4319/lo.2012.57.2.0519, 2012.

Cloern, J. E., Grenz, C., and Vidergar-Lucas, L.: An empirical model of the phytoplankton chlorophyll : carbon ratio-the conversion factor between productivity and growth rate, Limnol. Oceanogr., 40, 1313-1321, doi: 10.4319/lo.1995.40.7.1313, 1995.

Cloern, J. E., Abreu, P. C., Carstensen, J., Chauvaud, L., Elmgren, R., Grall, J., Greening, H., Johansson, J. O. R., Kahru, M., Sherwood, E. T., Xu, J., and Yin, K.: Human activities and climate variability drive fast-paced change across the world's estuarine–coastal 290 ecosystems, Glob. Change Biol., 22, 513-529, doi: 10.1111/gcb.13059, 2016.

Edwards, K. F., Thomas, M. K., Klausmeier, C. A., and Litchman, E.: Light and growth in marine phytoplankton: allometric, taxonomic, and environmental variation, Limnol. Oceanogr., 60, 540-552, doi: 10.1002/lno.10033, 2015.

Freilich, M., Mignot, A., Flierl, G., and Ferrari, R.: Grazing behavior and winter phytoplankton accumulation, Biogeosciences, 18, 5595-5607, doi: 10.5194/bg-18-5595-2021, 2021.

295 Geider, R. J.: Light and Temperature Dependence of the Carbon to Chlorophyll a Ratio in Microalgae and Cyanobacteria: Implications for Physiology and Growth of Phytoplankton, New Phytol., 106, 1-34, doi: 10.1111/j.1469-8137.1987.tb04788.x, 1987.

Hansen, P. J., Bjørnsen, P. K., and Hansen, B. W.: Zooplankton grazing and growth: Scaling within the 2-2,-μm body size range, Limnol. Oceanogr., 42, 687-704, doi: 10.4319/lo.1997.42.4.0687, 1997.

Haraguchi, L., Jakobsen, H. H., Lundholm, N., and Carstensen, J.: Phytoplankton Community Dynamic: A Driver for Ciliate Trophic 300 Strategies, Front. Mar. Sci., 5, doi: 10.3389/fmars.2018.00272, 2018.

Henson, S. A., Dunne, J. P., and Sarmiento, J. L.: Decadal variability in North Atlantic phytoplankton blooms, J. Geophys. Res. Oceans, 114, C04013, doi: 10.1029/2008JC005139, 2009.

Huisman, J., van Oostveen, P., and Weissing, F. J.: Critical depth and critical turbulence: two different mechanisms for the development of phytoplankton blooms, Limnol. Oceanogr., 44, 1781-1787, doi: 10.4319/lo.1999.44.7.1781, 1999.

305 León, P., Walsham, P., Bresnan, E., Hartman, S. E., Hughes, S., Mackenzie, K., and Webster, L.: Seasonal variability of the carbonate system and coccolithophore Emiliania huxleyi at a Scottish Coastal Observatory monitoring site, Estuar. Coast. Shelf Sci., 202, 302-314, doi: 10.1016/j.ecss.2018.01.011, 2018.

Lewandowska, A. M., Striebel, M., Feudel, U., Hillebrand, H., and Sommer, U.: The importance of phytoplankton trait variability in spring bloom formation, ICES J. Mar. Sci., 72, 1908-1915, doi: 10.1093/icesjms/fsv059, 2015.

310 Liu, K., Chen, B., Zheng, L., Su, S., Huang, B., Chen, M., and Liu, H.: What controls microzooplankton biomass and herbivory rate across marginal seas of China?, Limnol. Oceanogr., 66, 61-75, doi: 10.1002/lno.11588, 2021.

Mann, K. H.: Ecology of coastal waters: with implications for management, John Wiley & Sons, 2009.

Marine Scotland Science: Scottish Coastal Observatory - Stonehaven site data [dataset], doi: 10.7489/610-1, 2018.

Met Office: Met Office Integrated Data Archive System (MIDAS) Land and Marine Surface Stations Data (1853-current), NCAS British
315 Atmospheric Data Centre, 2021 [dataset], 2012.

Mignot, A., Ferrari, R., and Claustre, H.: Floats with bio-optical sensors reveal what processes trigger the North Atlantic bloom, Nat. Commun., 9, 190, doi: 10.1038/s41467-017-02143-6, 2018.

Mojica, K. D. A., Behrenfeld, M. J., Clay, M., and Brussaard, C. P. D.: Spring Accumulation Rates in North Atlantic Phytoplankton Communities Linked to Alterations in the Balance Between Division and Loss, 12, doi: 10.3389/fmicb.2021.706137, 2021.

320 Morison, F., Franzè, G., Harvey, E., and Menden-Deuer, S.: Light fluctuations are key in modulating plankton trophic dynamics and their impact on primary production, Limnol. Oceanogr. Lett., 5, 346-353, doi: 10.1002/lol2.10156, 2020.

R Core Team: R: A language and environment for statistical computing, available at: http://www.R-project.org/, 2020.

Reid, P. C., Lancelot, C., Gieskes, W. W. C., Hagmeier, E., and Weichart, G.: Phytoplankton of the North Sea and its dynamics: A review, Neth. J. Sea Res., 26, 295-331, doi: 10.1016/0077-7579(90)90094-W, 1990.

325 Rose, J. M. and Caron, D. A.: Does low temperature constrain the growth rates of heterotrophic protists? Evidence and implications for algal blooms in cold waters, Limnol. Oceanogr., 52, 886-895, doi: 10.4319/lo.2007.52.2.0886, 2007.

RStudio Team: RStudio: Integrated Development Environment for R, available at: http://www.rstudio.com/, 2020.

Simpson, J. H. and Sharples, J.: Introduction to the physical and biological oceanography of shelf seas, Cambridge University Press, 2012.

Sverdrup, H. U.: On conditions for the Vernal Blooming of Phytoplankton, J. Cons. Cons. Int. Explor. Mer., 18, 287-295, doi:
330 10.1093/icesjms/18.3.287, 1953.

Tarran, G. A. and Bruun, J. T.: Nanoplankton and picoplankton in the Western English Channel: abundance and seasonality from 2007–2013, Prog. Oceanogr., 137, 446-455, doi: 10.1016/j.pocean.2015.04.024, 2015.

Townsend, D. W., Cammen, L. M., Holligan, P. M., Campbell, D. E., and Pettigrew, N. R.: Causes and consequences of variability in the timing of spring phytoplankton blooms, Deep Sea Res. Part I Oceanogr. Res. Pap., 41, 747-765, doi: 10.1016/0967-
335 0637(94)90075-2, 1994.

Wickham, H., Averick, M., Bryan, J., Chang, W., McGowan, L. D., François, R., Grolemund, G., Hayes, A., Henry, L., Hester, J., Kuhn, M., Pedersen, T. L., Miller, E., Bache, S. M., Müller, K., Ooms, J., Robinson, D., Seidel, D. P., Spinu, V., Takahashi, K., Vaughan, D., Wilke, C., Woo, K., and Yutani, H.: Welcome to the Tidyverse, J. Open Source Softw., 4, 1686, doi: 10.21105/joss.01686., 2019.

340 Wilson, R. J. and Heath, M. R.: Increasing turbidity in the North Sea during the 20th century due to changing wave climate, Ocean Sci., 15, 1615-1625, doi: 10.5194/os-15-1615-2019, 2019.

Wood, S. N.: Generalized additive models: an introduction with R (2nd edition), Chapman and Hall/CRC, 2017.

Yang, B., Boss, E. S., Haëntjens, N., Long, M. C., Behrenfeld, M. J., Eveleth, R., and Doney, S. C.: Phytoplankton Phenology in the North Atlantic: Insights From Profiling Float Measurements, Front. Mar. Sci., 7, doi: 10.3389/fmars.2020.00139, 2020.

345